Removal of quinoline from oily wastewater using biochars prepared from compost

Giovanna Giacobbo Alves

Thesis report submitted to

School of Technology and Management

Polytechnic Institute of Bragança

Master Degree in

Chemical Engineering

Supervisors:

Prof. Dr. Helder T. Gomes

Prof. Drª Ana Maria F. Lima

Dr. Jose L. Diaz de Tuesta

Bragança

2019

Removal of quinoline from oily wastewater using biochars prepared from compost

Giovanna Giacobbo Alves

Thesis report submitted to

School of Technology and Management

Polytechnic Institute of Bragança

Master Degree in

Chemical Engineering

Supervisors:

Prof. Dr. Helder T. Gomes

Prof. Drª Ana Maria F. Lima

Dr. Jose L. Diaz de Tuesta

Bragança

2019

ACKNOWLEDGEMENTS

First of all, I would like to thank God for leading me on this new journey and for enlightening me in difficult times. To my parents for supporting me and providing this experience.

I would like to thank my supervisors, professor Dr. Helder T. Gomes of Instituto Politécnico de Bragança (IPB) and professor Dra. Ana Maria Ferrari Lima of Universidade Tecnológica Federal do Paraná (UTFPR). I really appreciate the opportunity, knowledge and trust given to me to carry out this work.

I would especially like to thank my supervisor Dr. Jose Luis Díaz de Tuesta for his patience, guidance, dedication and all assistance in the execution of this project. Without his help, this work would not have been accomplished, nor reformulated.

Lastly I would like to thank the UTFPR and IPB institutions, which gave me the opportunity to live this double degree, which made me grow personally and professionally. And for sure, they made me learn a lot every time I was here. I am very grateful for the trust placed in me.

This work is a result of the Project "AIProcMat@N2020 - Advanced Industrial Processes and Materials for a Sustainable Northern Region of Portugal 2020", with the reference NORTE-01-0145-FEDER-000006, supported by ERDF; and the Associate Laboratory LSRE-LCM - UID/EQU/50020/2019 - funded by national funds through FCT/MCTES (PIDDAC).

Abstract

The petrochemical industry is one of the main sources of aquatic pollution, because when its waste is discarded in water resources, the generation of oily wastewater is dangerous to the ecosystem and to human health. Due to the diversified origin of these waters they present an extremely varied composition and they are difficult to treat. Thus, this dissertation aims to evaluate the removal of quinoline, a compound derived from the petrochemical industry, through an adsorption process. A solution of quinoline solubilized in 2,2,4-trimethylpentane was used as pollutant solution. Three different types of activated carbons prepared from precursor mixtures of compost originated from urban solid waste and glycerol were used as adsorbents and their adsorption capacity was tested. The adsorption kinetics of quinoline reveal that the adsorption is very fast in the first 30 minutes and that this process is more efficient at low concentrations. The kinetic data for the three activated carbons were successfully fitted to the pseudo-second order model. The equilibrium data were better adjusted to the Freundlich model, revealing the adsorption process physisorption character. The maximum adsorption capacity obtained by the Langmuir model was 3.376 $mg \cdot g^{-1}$. The results show that activated carbons with ratios of compost:glycerol of 1:3 (C_1G_3) and 2:2 (C_2G_2) were the best adsorbents.

Resumo

A indústria petroquímica é uma das principais fontes de poluição aquática, pois quando os seus resíduos são descartados nos recursos hídricos ocorre a geração de águas residuais oleosas que são perigosas para o ecossistema e para a saúde humana. Devido à origem diversificada destas águas elas apresentam uma composição extremamente variada e de difícil tratamento. Assim, esta dissertação teve como objetivo avaliar a remoção de quinolina, um composto derivado da indústria petroquímica, por meio de um processo de adsorção. Uma solução de quinolina solubilizada em 2,2,4-trimetilpentano foi utilizado como solução poluente. Foram utilizados como adsorvente três tipos diferentes de carvão ativado preparados a partir de misturas de resíduos sólidos urbanos e glicerol, avaliando-se a sua capacidade de adsorção. A cinética de adsorção da quinolina revelou que nos primeiros 30 minutos a adsorção é muito rápida e que este processo é mais eficiente em concentrações baixas. Os dados cinéticos para os três carvões ativados foram ajustados com sucesso ao modelo de pseudo-segunda ordem. Os dados de equilíbrio foram mais bem ajustados ao modelo de Freundlich, revelando o caráter de fisissorção do processo de adsorção. A capacidade de adsorção máxima, obtida através do modelo de Langmuir, foi de 3.376 $mg \cdot g^{-1}$. Os resultados mostram que os carvões ativados preparados com razões composto:glicerol de 1:3 (C_1G_3) e 2:2 (C_2G_2) foram os melhores adsorventes.

List of Figures

List of Tables

Summary

INTRODUCTION

1 INTRODUCTION

The increasing global energy demand, which is expected to be 44% over the next two decades, makes the processing of petroleum, a complex mixture of organic liquids called crude oil and natural gas[1], one of the main sources of energy in the world, since the world energy matrix still has its basis in the consumption of fossil fuels[2].

However, one of the consequences of increasing oil production is the high generation of oily wastewater originating from the petroleum industry, petroleum refining, petroleum storage industries, transportation and petrochemical industries, which are subsequently released into the natural environment, creating a large ecological problem around the world[2–4].

The pollution of these oily wastewater is mainly manifested in the following aspects: (1) affecting drinking water and groundwater resources, endangering aquatic resources; (2) endangering human health; (3) atmospheric pollution; (4) affecting crop production; (5) destructing the natural landscape.[3,4].

As these oily wastewaters are generated by different industries, their composition is very varied and therefore the treatment of this water requires techniques that support the whole range of waste generated[2]. Therefore, the treatment system used should be able to treat the effluent so that no unnecessary waste is generated during the treatment process. In addition, the treatment should be free from noise and odor disturbances, nor cause negative environmental impact[5], and must comply with local waste disposal regulations imposed by local, national and international authorities[6].

All of these problems and environmental concern promoted the development of new processes for oily wastewater treatment, since the conventional oily wastewater treatment methods, such as gravity separation, flotation and chemical coagulation remain unsatisfactory, presenting several disadvantages like low efficiency, high operation costs, corrosion and recontamination problems, among others. The physical–chemical treatment has emerged as a new alternative due to several advantages: no chemical additives are needed to break the emulsion, high chemical oxygen demand removal efficiencies are achieved and treatment facilities are quite compact and fully automated. Many methods and techniques, such as coalescence, membrane separation and adsorption, which were shown to be prominent, have been developed to deal with oily wastewater[3,6].

In this context, the adsorption process for the treatment of oily wastewater with activated carbons is an alternative scarcely explored[4], but looks like promising because it is considered as the most economical and efficient process for the removal of organic compounds in dilute aqueous solutions. Activated carbon adsorption has been cited by the USEPA as one of the best available environmental control technologies. Activated carbons are profusely used as adsorbents for decontamination processes because of their extended surface area, high adsorption capacity, microporous structure and special surface reactivity[7].

The current work is focused on the removal of lipophilic pollutants, such as quinolone, from organic phase and two-phase systems (simulating contamination of oil-water mixtures) using as adsorbents different activated carbons prepared from compost originating from municipal solid waste.

STATE OF THE ART

2 STATE OF THE ART

2.1 WATER ISSUES

The present development model of our societies, population growth and increasing industrialization is making the humanity to face problems such as water scarcity that have become a threat to human health and life on the planet. Due to economic, political and climatic reasons, 40% of the world population is affected by lack or scarcity of water and more than 25% of the population suffers from health problems or hygiene related to water. 1.1 billions of people do not have access to adequate sources of water, specially in poorer countries such as in Africa, Asia and Latin American countries[8]. In parallel, the domestic use and the industrial activities, mainly in developed countries, generate high amounts of waste and effluents that generally are discarded directly into natural water courses, attacking the environment and giving rise to wastewater. A water effluent whose physical, chemical or biological properties have been changed due to the introduction of certain substances, which render it unsafe for some purposes, such as for drinking is considered an wastewater[9]. The discharge of this wastewater in the soil can cause contamination of the groundwater or the accumulation of toxic products in plants and animals, which can result in the destruction of the aquatic life existing in the place of contamination. Therefore, the planet needs environmental preservation, and it is extremely necessary to reduce the quantity or to improve the quality of effluents discarded in the bodies of water[8,10].

In contrast to this need for environmental preservation, industrial growth is increasing, resulting in increased demand for fuel and energy, consequently in a greater demand for petroleum and gas production. However, these petroleum and gas production processes generate large volumes of liquid waste[1,11]. These wastewater, unwanted by-products associated with petroleum and gas extraction[1], are known as oily wastewater, and considers all types of water containing varying amounts of oils (mineral, vegetable or synthetic), greases, lubricants, fatty acids, emulsifiers, corrosion inhibitors, bactericides and other materials derived from petroleum or oils[2,10]. Their main contaminating components includes light hydrocarbons, heavy hydrocarbons, oil, tar, lubricating oil, fatty oils, wax oils, soaps, among others[12]. Sources of such oily wastewater is very broad, but it is mainly generated from oil processing, petrochemical, metallurgical and mechanical industries and maritime transport[12]. The composition and characteristics

of these waters varies greatly according to their origin, and the oil content can be either low or very high[5].

According to statistics, every year at least 500 to 1000 million tons of oil is discharged into the water through a variety of ways[12], such as in the production, transport, refining or during the use of its derivatives. Due to this large quantity of petroleum discharged in the water, this became a major source of aquatic environmental pollution[1]. As consequence it affects drinking water, groundwater resources and several ecosystems, since the presence of oils result in damage to the aeration and natural illumination of watercourses, due to the formation of an insoluble film in the surface, producing harmful effects on aquatic life and causing death of animal and plants[10,13]. It also endangers human health, pollutes the atmosphere, affects agricultural production, destroys the natural landscape, among other[12]. To combat the large amount of oily effluents generated each year and the associated costs of these waters, companies have sought to improve their treatment of effluents, seeking the application of new technologies and the improvement of the already existing treatments, that allow the framing of the effluents to the legal requirements[1]. The treatment of these oily effluents can be regarded not only as a decontamination need of the waters, but also as an opportunity to remove and recover organic pollutants from the oily fraction of the oily wastewater, to be used as a potential organic fuel, lubricant or other raw material[4].

Environmental control agencies have reviewed the current laws and imposed stricter limits on the disposal of effluents[10]. Currently, the new defined and permitted limits of oil and grease for the discharge of water produced and treated at sea in Brazil are 42 $mg \cdot L^{-1}$ per day at maximum and the monthly average limit is 29 $mg \cdot L^{-1}$ as defined by CONAMA, 2009 (article 24º of Conama 357)[5]. And these are the same limits permitted by the United States Environmental Protection Agency (USEPA)[11]. In Portugal, these limits are defined by Law n.º 58/2005, of December 2009, which follows the Directives 2000/60/CE of the European Parliament and of the Council of 23 October of 2005[14].

The treatment of oily wastewater is necessary in order to meet environmental disposal standards and/or the characteristics required for water reuse and avoid its impact on the environment. One of these effluents that is found in oily wastewater from various petrochemical sectors is quinoline, a compound derived from petroleum that has a nitrogen atom in its structure making it dangerous to human health and therefore its treatment is necessary.

2.2 QUINOLINE

Oily wastewater effluents can be contaminated with small amounts of nitrogen, sulfur and metal compounds. These compounds, specially nitrogen ones, are of great environmentally and technologically important, because they are considered carcinogenic, mutagenic and difficult to treat, thus representing a great risk associated with dispersion to the atmosphere[15,16]. The compounds of nitrogen can be classified in basics and neutrals. Examples of basic compounds are quinoline, pyridine and pyrrole. Examples of neutral compounds are indole and carbazole[16].

Quinoline (Figure 1) is an hygroscopic liquid that is colorless, has a pungent odor, darkens with age and is a weak tertiary base derived from naphthalene[17]. The quinoline belongs to the group of PNA-compounds (poly nuclear aromatics) being a heterocyclic compound[18,19].

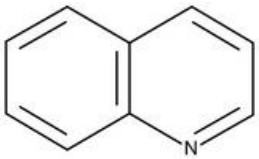

Figure 1 - Chemical structure of quinoline.

Quinoline is widely produced by the refining of petroleum, being also found in the processing of coal effluents, shale and different fuel oils. In the petroleum refining process, it can adsorb strongly in the acid sites of the catalysts used in the petroleum refining process, causing the poisoning of the active sites. Therefore, these compounds are considered contaminants of the process and must be removed prior to the conversion steps to obtain light derivatives[20].

Quinoline is also widely used as an intermediary in the metallurgical industry, in the production of dyes, polymers and agricultural chemicals, besides being a primordial solvent of resins and terpenes. Due to the diversity of applications of quinoline[17,21], it can be found in ground waters, therefore being in the group of important environmental contaminants[15].

Due to the presence of a N atom embedded in the quinoline ring system, its solubility in water (6 $g \cdot L^{-1}$)[22] is markedly increased, thus increasing its bioavailability[18]. The rate of biodegradation depends on factors such as temperature and microbial

conditions[17], but this rate is low, which is reflected in the considerable amounts of quinoline found in the ground water of the gasification sites[15] (in $mg \cdot L^{-1}$ levels)[18]. Quinoline is biologically transformed to 2-hydroxyquinoline, whereas further biological processes apparently take place only very slowly[18]. When released to soil, quinoline is likely to leach quickly into groundwater[17]. With the low rates of degradation of quinoline and its toxicity, traditional methods to treat oily wastewater containing quinoline are often not as efficient[15].

2.3 TREATMENT OF OILY WASTEWATER

Several strategies and practical solutions have been adopted to generate more viable water resources from the treatment of oily wastewater[23]. However, the actual removal of all substances present in the effluents by means of treatment of waters is a challenge, due to the variety of forms in which the oil can be contained in the waters[23], specifically in four different forms: free, emulsified, dispersed and solubilized [5].

Several conventional oil/water separation processes are presently known, but the choice of the appropriate method depends on the characteristics of the effluent, in the form in which the oil/water interaction occurs, the size of the dispersed oil droplets, the suspended solids content and oil concentration[10]. The techniques for the treatment of oily wastewater can be divided into physical, chemical, physical-chemical, biological, mechanical and electrical, and can be used together according to the type of effluent and the purpose of the treatment[5].

Of all these treatment techniques, we can mention several treatment methods that have been used such as coagulation/flocculation, biological treatment, adsorption, electrochemical treatment, early oxidation process, membrane process. However, due to the toxicity of quinoline, the biological treatment is not suitable for such wastewater[24].

Thus, the adsorption process has demonstrated to be an attractive method for the removal of organic compounds, such as quinoline. This process eliminates the need for huge sludge handling processes[25]. This type of treatment is usually carried out with activated carbon and has attracted academic interest because it is a low cost, efficient and easy to use process[26,27], and activated carbon is an adsorbent capable to remove refractory, toxic, non-biodegradable and pharmaceutical compounds, compounds derived

from petroleum, among others[28]. Therefore, several authors have reported in literature the removal of quinoline by means of several types of adsorbents.

2.4 ADSORPTION

The adsorption was first observed by C.W.Scheele in 1773 for gases and then for solutions by Lowitz in 1785[29]. Adsorption is a mass transfer process of the solid-fluid type[30], where occurs the accumulation and selective concentration of one or more fluids on the solid surface. The material on which the adsorption occurs is named adsorbent, and the adsorbed substance is the adsorbate, which may be a liquid or gaseous substance immersed in a fluid[31]. The formation of an adsorbed layer on a surface does not occur in an instantaneous process[32], but is formed as the molecules present in this fluid are attracted to the interfacial zone by the existence of unbalanced attractive forces on the surface of the adsorbent[33].

The adsorption is a process that occurs in four stages represented in Figure 2 following the respective order: contact, adsorption on the outer surface, diffusion and adsorption at the internal sites of the solid[34].

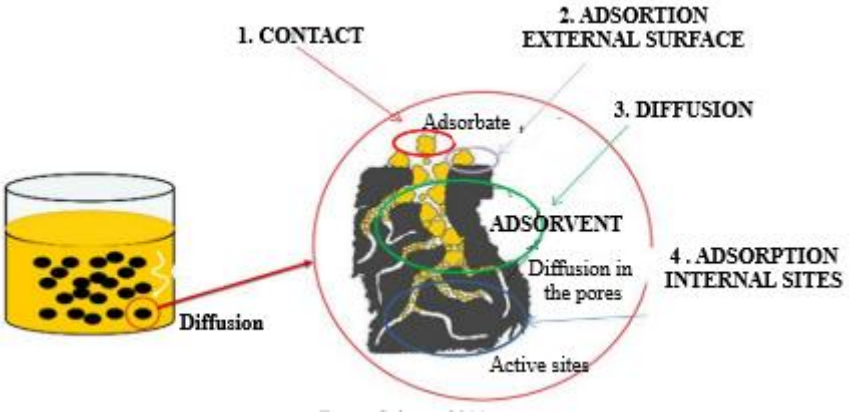

Figure 2 - Adsorption system[34].

Adsorption process can be explained by four steps. First, the contact between adsorbate molecules and the outer surface of the adsorbent takes place, this characteristic has to occur rapidly and depends on the initial concentration of the aqueous medium. Secondly, the adsorption occurs on the outer surface of the solid, being dependent on the nature of the adsorbent and the adsorbate[34]. In the third stage, the diffusion of adsorbate

molecules in the pores occurs (intraparticle diffusion). This mechanism is favored in solids of greater porosity favoring adsorbates of great molecular mass and/or with functional groups with high load. Generally, diffusion is the controlling step, due to the difficulty in mobility of the molecules. The fourth and final stage adsorption of adsorbate molecules occurs at the available sites on the inner surface[34].

There are different parameters affecting adsorption processes. A very important parameter for adsorption is the surface area of the adsorbent, because the larger the surface, the more unbalanced forces are available, favoring adsorption[31]. Usually the amount of material adsorbed varies from 5 % to 30 % of the weight of the adsorbent, and can reach 50 %[34,35].

The type of interaction between the adsorbed material and the surface of the adsorbent is another important feature for the adsorption process, since it is responsible for determining the nature of the adsorption which may be chemical or physical[35]. Physical adsorption occurs when intermolecular forces of attraction of molecules in the fluid phase and the solid surface are larger than the attractive forces between the molecules of the fluid itself, that type is the most common[30,31]. These intermolecular forces are weak, mainly Van der Waals forces or electrostatic forces such as polarization and dipole[32]. This type of adsorption is reversible, not specific, is a rapid process and is generally limited by diffusion phenomena, and there may be formation of multiple layers of adsorption and the adsorption heats are low[35].

In chemical adsorption, there is the involvement of chemical interactions between adsorbate and adsorbent, resulting from the transfer of electrons, equivalent to the formation of chemical bonds between the adsorbate and the surface of the solid[31,32]. The adsorbate undergoes a chemical change and is generally dissociated into independent fragments, forming radicals and atoms attached to the adsorbent[30]. This type of adsorption is very specific and is accompanied by a strong variation of the activation energy, occurring generally at temperatures above the boiling point of the liquid adsorption medium[35]. In this case, the heat of adsorption is of the same order of magnitude of the heats of chemical reactions[32].

2.4.1 ADSORPTION ISOTHERMS

The solute distribution between the adsorbed phase and the liquid phase as well as all phase equilibria is dependent on the principles of thermodynamics[36]. Adsorption equilibrium is reached when the adsorption velocity is equal to the desorption velocity, and at a given[37] temperature and pressure depends on several factors such as the nature of the solid (active sites, pore distribution, among others) and nature of the adsorbate (type of adsorbent / adsorbate interaction and molecular size) [36].

The phase equilibrium thus constitutes one of the most important parameters for the adsorption study being known as adsorption isotherms. It is a curve obtained from the equilibrium relation between the amounts of solute adsorbed as a function of the concentration of this solute in the solution at a defined temperature[38,39]. These curves allow to study how a component is accommodated by solid adsorbent[38].

From the isotherms many, data can be known in relation to the adsorption process, such as how the adsorbent effectively adsorbs the impurities present in the effluent and if the desired purification can be obtained[32], estimate the maximum amount of impurities that will be adsorbed, and thus to evaluate the use of a particular adsorbent in the removal of a specific contaminant during the treatment of effluents, to evaluate the adsorbent/adsorbate affinity , among other factors[32,34].

Several types of isotherms are known and currently used, one of these isotherms was proposed by Giles et al (1960)[40] where the isotherms were divided in four main classes according to the initial slope and each class was subdivided in various subgroups, based on the shape of the upper parts of the curve. The four classes were named of isotherms of type S (“Spherical”), L (“Langmuir”), H (“High affinity”) ad C (“Constant partition”)[34,41]. The Giles isotherms can be verified in Figure 3.

The type S isotherms (Spherical) have a linear and convex slope in relation to the abscissa, because the adsorbent/adsorbate interactions are weaker than the adsorbate/ adsorbate and solvent/adsorbent interactions[41]. Due to this low interaction the initial adsorption is low and increases with the number of molecules adsorbed, indicating that an association occurs between adsorbed molecules, called cooperative adsorption[34,39].

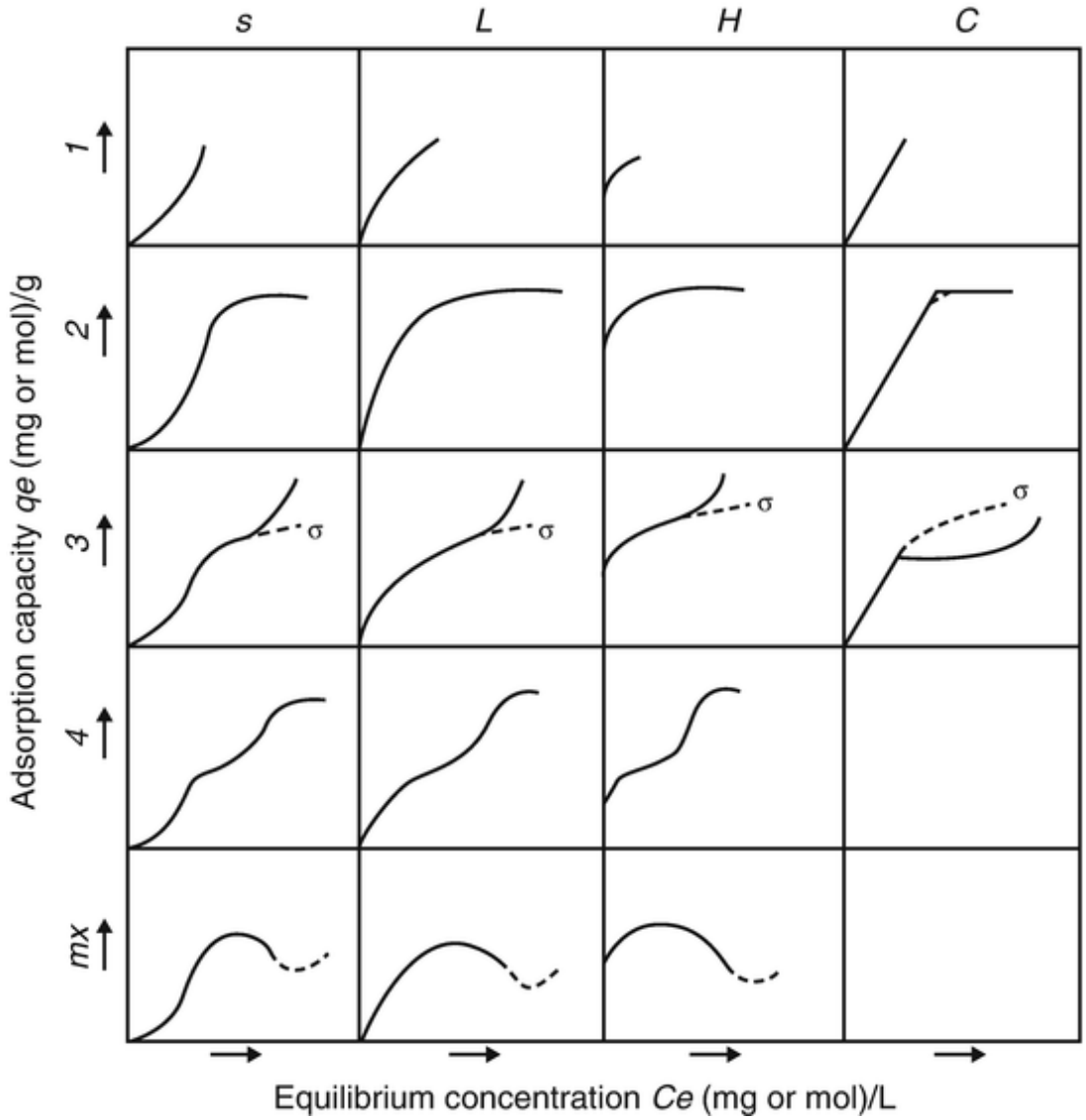

Figure 3 - Isotherms of Giles[42].

The type L isotherm (Langmuir) has a non-linear and concave slope in relation to the abscissa, demonstrating that in this case, there is high affinity between the adsorbent for the solute at low concentrations[41]. In this type of isotherm it is verified that a decrease of the availability of the adsorption sites occurs with the increase of the concentration of the solution[32,39].

The type H isotherms (High-affinity) are a special case of L type isotherms which are observed when the surface of the adsorbent has high affinity for the adsorbed solute. The initial adsorbed amount is high and soon after equilibrium is reached[39,41].

The type C isotherms (Constant partition) correspond to a constant partition of the solute between the solution and the adsorbent, giving the curve a linear aspect. This

type of curve is obtained for partitioning a solute into two immiscible solvents[32,41]. The conditions favoring the type C curves are flexible porous substrates and regions of different degrees of solubility for the solute. The isotherms of type C and L are very close and can be, in some situations, considered of the same type[34,39].

The subgroup 2 represents the isotherms that have surface saturation in which the adsorbate has more affinity for the solvent than for the adsorbed molecules. Subgroup 3 is characterized by a rise after an inflection point. The subgroup 4 indicates that there is formation of multiple layers. Finally, the subgroup mx shows that the isotherm shows a maximum at high concentrations. It is a rare case and indicates that at high concentrations of adsorbate the adsorbate/adsorbate interactions increase much faster than the adsorbate - adsorbent attractions[32].

2.4.2 ISOTHERM ADSORPTION MODELS

Besides the classification of Giles the isotherms can still be classified according to some models the most know and used, were proposed by Langmuir and Freundlich. In 1916 Irving Langmuir developed the Langmuir model that was proposed to describe the adsorption of gases in solids, being based on [30,43] the following assumptions (i) only one monolayer of adsorbate on the surface of solid is formed; (ii) there is a defined number of sites; (iii) the adsorption process occurs without any interaction between adsorbed molecules; (iv) the adsorbent has a surface with identical and energetically equivalent sites[31,44].

By assuming that the solvent and solute molecules occupy the same area when adsorbed on the surface of the adsorbent upon reaching equilibrium, the rate of adsorption and desorption become equal. This model has been used successfully and presents good results for adsorption in solids with large surface area and the Langmuir model can be represented by Eq. (1)[45].

$$q_e = \frac{q_m k_L C_e}{1 + (k_L C_e)} \quad (1)$$

Where q_e is the quantity adsorbed ($mg \cdot g^{-1}$) to a concentration of the adsorbate; q_m is the maximum adsorption capacity ($mg \cdot g^{-1}$); C_e is the concentration of adsorbate in equilibrium ($mg \cdot L^{-1}$) and k_L is the constant of Langmuir.

Different from the Langmuir model, the model proposed by Herbert Max Finley Freundlich is an empirical model that considers the adsorption in several layers on a heterogeneous surface. The Freundlich equation suggests that the adsorption energy decreases logarithmically as the surface becomes covered by the solute, being described by Eq. (2)[46].

$$q_e = k_F C_e^{1/n} \quad (2)$$

Where q_e is the quantity adsorbed ($mg \cdot g^{-1}$) to a concentration of the adsorbate; C_e it is the concentration of adsorbate in equilibrium ($mg \cdot L^{-1}$) and k_F it [$(mg \cdot g^{-1})(L \cdot mg^{-1})^{1/n}$] and n are the constants of Freundlich. k_F represents the adsorption capacity while n represent the intensity of the adsorption process, a favorable adsorption tends to have a value of n between 1 and 10[47]. The smaller the value 1/n the stronger the interaction between the adsorbent and the adsorbate, the higher the value 1/n the more unfavorable is the adsorption and when the value of 1/n is equal to 1 the adsorption is linear and the energies are identical for all the adsorption sites[45].

2.4.3 ADSORPTION KINETICS

The equilibrium analysis is fundamental to evaluate the affinity and the capacity of an adsorbent. However, these data only predict the final state of a system that was initially not in equilibrium[48]. Therefore, a study of adsorption kinetics is particularly significant because it provides valuable information about the reaction pathways and into the mechanism of adsorption reactions[25].

The kinetic term deals with changes in the chemical or physical properties of the process over time[38], that is, it describes the rate at which the adsorbate molecules are retained by the adsorbent, representing how much was withdrawn from the solution with respect to time and the efficiency of the adsorbate[26,34].

Some factors directly affect adsorption kinetics, which may be related to adsorbate, adsorbent and solution. In relation to adsorbate, these factors are related to molar mass, solubility and particle size. In relation to the adsorbent, pore structure and the available surface area; and in relation to the aqueous solution or effluent the important factors are pH, temperature and initial concentration[49].

To develop adsorption kinetics, a knowledge of the rate law describing the adsorption system is required. The rate law is determined by experimentation and it cannot be inferred by examination of the overall chemical reaction equation[25]. The rate law takes into account steps:

- Adsorbate molecules are transported from the liquid phase through the boundary layer surrounding the adsorbent[37,38];
- Intraparticle diffusion: transfer of adsorbate from the surface to the active sites inside the particles[37,38];
- Adsorption finally occurs the adsorption of solute molecules on the surface of the adsorbent's internal pores[37,38].

Several kinetic models for data analysis have been proposed in the literature, the main ones being the pseudo first order model and the pseudo second order model.

2.4.3.1 PSEUDO FIRST ORDER MODEL

The model of pseudo-first-order was proposed by Lagergren in 1898. It is widely used in adsorption processes and is based on the adsorption capacity of the solid[39,50]. The equation of this model considers that the driving force is the difference between the amount of solute adsorbed at equilibrium and the amount of solute adsorbed at a given time (t), as follows by Eq. (3)[26,37].

$$\frac{dq_t}{dt} = k_{p1}(q_e - q_t) \quad (3)$$

Where $k_{p1}$is the pseudo-first-order rate constant, q_t is the amount of solute adsorbed at time t and q_e is the amount of solute adsorbed in the equilibrium[32,50]. In many

cases, the Lagergren equation does not fit well for any contact time range, as it is only applicable to initial stages of adsorption, usually between the initial 20-30 minutes[48,51]. The adsorption rate is determined by Eq (4).

$$q = q_e(1 - exp^{-k_{p1}t}) \quad (4)$$

2.4.3.2 PSEUDO SECOND ORDER MODEL

This model considers that the rate depends on the adsorption capacity and not the adsorbate concentration, assuming that the adsorption capacity is proportional to the number of active centers occupied on the surface of the adsorbent[48], reporting the behavior of the process over the entire time interval, in opposition to the Langergren model. The model predicts behavior throughout the study range[39,51].

$$\frac{dq_t}{dt} = k_{p2} \times (q_e - q_t)^2 \quad (5)$$

Where k_{p2} is the pseudo-second-order rate constant, q_t is the amount of solute adsorbed at time t and q_e is the amount of solute adsorbed in the equilibrium. The adsorption rate is determined by Eq (6).

$$q = \frac{k_{p2}q_e^2 t}{1 + k_{p2}q_e t} \quad (6)$$

2.4.4 ACTIVATED CARBON AS ADSORBENT

The presence and importance of activated carbon into the human history extends so far back in time that its origin is impossible to be accurately determined[35]. The activated carbon is used by humanity since very time where, the first recorded case dates back to 3750 BCE, when both the Egyptians and Sumerians used wood char for the reduction of copper, zinc and tin ores in the manufacturing of bronze, and also as a smokeless fuel[43,52]. The rapid development of modern society over the 20th century promoted a fast growing production and utilization of activated carbon, especially after the First World War where the same was used against toxic gases[53,54].

Later the use of activated carbon has become increasingly large due to the stricter environmental regulations regarding water resources, clean gas application, air quality control, energy storage/conversion and economic recovery of valued chemicals. In addition, the search of an alternative use for several agro industrial waste, besides the replacement of petroleum-derived products, helped a increase in the use of activated carbon[52]. In addition, nowadays, activated carbon is almost exclusively use as adsorbent.

Activated carbon is defined as an inert carbonaceous material obtained from substances with high carbon content and subjected to special treatment to create a highly porous microcrystalline structure that provides a large surface area, which gives it the ability to adsorb molecules present in both liquid and gas phase[28,53]. Being a non-graphitic material, it has a small amount of heteroatoms, mainly oxygen, bound to the carbon atoms. Its properties depend on the raw material, the process and the activation time used, besides the final form of the coal[43]. There are several forms of activated carbon such as powdered coal (PACs), granulated (GACs), activated carbon fibers (ACFs), carbon monoliths or spherical activated carbons with their different applications[52,55].

As the basis of this material is the carbon, the activated charcoal can be manufactured from various materials, long as the raw material contains a high percentage of carbon. Raw materials used in coal production may be of vegetable origin (such as wood, peat, seeds, coconut shells and nuts), animal (such as animal bones) or mineral (such as petroleum, coal, plastic, tires, lignite and bituminous material)[53,55]. However, some characteristics must be taken into account when choosing the source material, for example the material should be rich in carbon and low inorganic content. Other important factors to be consider as are the cost and availability of the source material. For the activation of the carbon, two groups are currently known to be chemical activation and physical activation[43].

To be used with adsorbent, the activated carbon must have a high surface area, and the performance of the activated carbons as adsorbents depends strongly on its textural properties, such as, porosity, pore width, pore distribution and specific surface area[55,56]. According to the International Union of Pure and Applied Chemistry (IUPAC), activated carbon can be classified into three main groups according to the pore diameter (Table 1) [43].

Table 1- IUPAC classification of pores and function[54].

Porous Classification	Porous Diameter	Function
Microporous	$\theta_m < 2\ nm$	Provides a high adsorption capacity for small molecules such as common gases and solvents.
Mesoporous	$2\ nm < \theta_m < 50\ nm$	Used in the adsorption of large molecules, such as dyes. In addition, it provides part of the surface are for carbons impregnated with chemicals.
Macroporous	$\theta_m > 50\ nm$	It has the function of transport medium for gas molecules.

Although most of the adsorption occurs in the microporous of the activated carbon, mesoporous and macroporous play important roles in the adsorption process because they serve as the passage of the adsorbate to the microporous, which are mostly found inside the coal particle.

MATERIAL AND METHODS

3 MATERIAL AND METHODS

3.1 REAGENTS

Quinoline (98%. Alfa Aesar, C_9H_7N) was used as pollutant model and 2,2,4-trimethylpentane (99.9%. VWR Chemicals, C_8H_{18}) as solvent. Aliquots were prepared through dilution of the samples using ethanol (99.8%. Ficher Chemical, C_2H_6O) with analytical grade as solvent.

Glycerol (>99%. Cymit Quimica, S.L, $C_3H_8O_3$) and sulphuric acid (98%. Labkem, H_2SO_4) were used in the preparation of the biochars prepared from compost, used as precursors, that was supplied by the company Resíduos do Nordeste, EIM. The characterization of the compost is summarized in Table 2.

Sodium Hydroxide (98.76%. Fisher Chemical, NaOH), hydrochloric acid (37%, Fisher Chemical, HCl), distillated water and phenolphthalein were used in solution for the determination of surface groups.

Table 2 - Properties of the material used in the synthesis of activated carbons from the company "Resíduos do Nordeste, EIM" and based on standard analytical techniques[56].

Moisture	29.6%
Organic Matter	48.8%
Organic Carbon	27.1%
Nitrogen (N)	1.3%
Phosphorus (P_2O_5)	1.1%
Potassium (K_2O)	1.4%
Calcium (Ca)	4.9%
Magnesium (Mg)	0.8%
Sulphur (S)	0.6%
Boron (B)	43.4 mg/kg
Cadmium (Cd)	0.9 mg/kg
Chromium (Cr)	130 mg/kg
Copper (Cu)	209.7 mg/kg
Mercury (Hg)	0.4 mg/kg
Nickel (Ni)	49 mg/kg
Lead (Pb)	110 mg/kg
Zinc (Zn)	453 mg/kg
Salmonella spp. (in 25 g of fhesh matter)	Off
Escherichia coli (n°/g of fhesh matter)	460
Density	0.45 kg/dm^3
Electric conductivity	2.5 mS/cm
pH (in fresh matter)	8.0

3.2 PREPARATION OF MATERIALS

Adsorbent material were taken from a previous work. It was prepared from glycerol and compost. The compost derived from the mechanical biological treatment of the organic fraction of municipal solid waste, as alternative solution to valorize it. In this sense the activated carbons used were prepared from the residue described in **Table 2**.

The materials were synthesized from a mixture of glycerol, compost and sulfuric acid (40 g). The suspension was gently heated and exposed to 800 ºC for 20 min to allow in situ partial carbonization. The mass ratio of glycerol and compost were varied in 3 reactions, with the amounts of these components resulting in 20 g[56]. The mass ratio of reactions with glycerol and compound are described in sequences and the biochars synthesized were used in the form of particles with a diameter of 250 µm – 160 µm:

1) C_1G_3 from carbon materials and glycerol in a ratio 1:3;
2) C_2G_2 from carbon materials and glycerol in a ratio 2:2;
3) C_3G_1 from carbon materials and glycerol in a ratio 3:1;

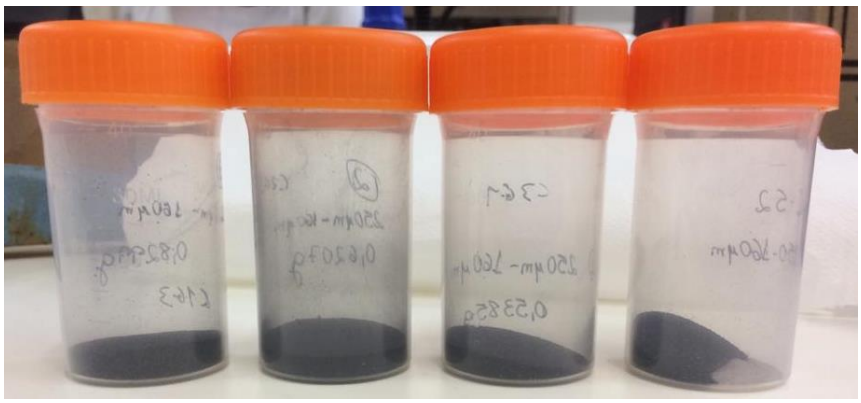

Figure 4 – Biochar samples.

The elemental composition of the biochars used were determined by a Carlo Erba EA 1108 Elemental Analyser and their textural properties were previously analyzed by a Quantachrome instrument NOVA TOUCH LX adsorption analyzer. adsorption analyzer are found in Table 3 and **Erro! Fonte de referência não encontrada.**Table 4.

Table 3 – Elemental composition of biochars [56].

Material	N (%)	C (%)	H (%)	S (%)	Remaining (%)
C_1G_3	0.02	74.44	0.65	0.99	23.8
C_2G_2	0.60	53.25	0.94	1.40	43.7
C_3G_1	0.02	33.87	0.28	2.30	63.5

Table 4 – Textural properties of activated carbon[56].

Material	S_{BET} ($m^2 \cdot g^{-1}$)*	S_{EXT} ($m^2 \cdot g^{-1}$)*	S_{mic} ($m^2 \cdot g^{-1}$)*	V_T ($cm^3 \cdot g^{-1}$)*
C_1G_3	8	8	0.51	7.9
C_2G_2	14.03	14.03	0.00	15.0
C_3G_1	14.13	14.13	0.00	21.9

*S_{BET}: BET surface area; S_{EXT}: external surface area; S_{mic}: surface area of microporous; V_T: total pore volume

3.3 DETERMINATION OF ACIDITY AND BASICITY

Quantification of surface acidic and basic functional groups was performed[57]. For this purpose, solutions of 0.02 mol·L^{-1} HCl and 0.02 mol·L^{-1} NaOH were prepared.

In an erlenmeyer of 100 mL containing 0.2 g of each biochar sample, 25 mL of HCl or NaOH solutions was added separately for the determination of the basicity and acidity, respectively. The resulting suspensions were allowed to stir for 48 h at room temperature on an orbital shaker (IKA®KS 130 basic). After 48 h the samples were filtered on filters (150 mm, Prat Dumas France) to remove solid material. In order to determine the acidity of material, 20 mL of filtrated NaOH solution was taken and titrated with 0.02 mol·L^{-1} HCl solution for quantification of unreacted hydroxyl (OH^-), using phenolphthalein as indicator. The initial concentration of functional acids was calculated by Eq. (7). The basicity of the samples was determined by taken 20 mL of the filtrated HCl solution, which was titrated with 0.02 mol·L^{-1} NaOH solution, using phenolphthalein as an indicator. The initial concentration of the functional base was calculated by Eq. (8):

$$Q_A = \frac{(V_W - V_t)MV_0}{V_{al}W} \quad (7)$$

Where Q_A is the quantity of acid groups in mol·g^{-1}, V_w is the volume to titrate the blank (mL), V_t is the volume used to titrate the sample (mL), M is the actual concentration of the NaOH or HCl solution (mol·L^{-1}), V_0 is the volume of solution initially used (L), V_{al} is the volume of the aliquot taken from the filtered (mL) and W is the mass of the sample (g).

$$Q_B = \frac{(V_W - V_t)MV_0}{V_{al}W} \quad (8)$$

Where Q_B is a quantity of basic groups in mol·g^{-1}, V_w is the volume to titrate the blank (mL), V_t is the volume used to titrate the sample (mL), M is the actual concentration of the NaOH or HCl solution (mol·L^{-1}), V_0 is the volume of solution initially used (L), V_{al} is the volume of the aliquot taken from the filtered (mL) and W is the mass of the sample (g).

3.4 ADSORPTION OF QUINOLINE

The experiments were carried out on an orbital shaker and agitation at the following conditions: (1) quinoline solution 20 mL; (2) biochars mass 50 mg resulting in initial solid material concentration 2.5 mg·L^{-1}; (3) stirring at 320 rpm and (4) total experiment time 4 hours.

The biochars were weighted and then sealed, so that they would not adsorb any pollutants that might be in the air. After weighing, the quinoline solution in 2,2,4-trimethylpentane to be treated was added in a volume of 20 mL to each 100 mL capacity erlenmeyer at varying concentrations of 2 to 120 mg·L^{-1} of quinoline at ambient temperature. The erlenmeyers were arranged afterward on the orbital shaker (IKA®KS 130 basic). Samples were collected at the times of 10, 20, 30, 60, 240 and 480 minutes and stored in *vials* for further spectroscopic analysis.

Figure 5 - Quinoline adsorption experiment.

The adsorption equilibrium study was carried out in continuation of the study of adsorption kinetics. After the first part of the experiment, the samples were allowed to stir until they had completed 72 h of experiment and consequently reached equilibrium.

3.5 ANALITYCAL METHODS

3.5.1 QUINOLINE DETERMINATION

To monitor the adsorption of quinoline on the biochar adsorbent, the samples collected during the adsorption runs were diluted in ethanol in a ratio 1:5 in volume and then analyzed by UV-VIS spectrophotometry (JASCO, V-530 spectrometer) at the wavelength of 300 nm. A standard curve with different aliquots of quinoline at solved in 2,2,4-trimethylpentane and ethanol was performed (**Figure 6**).

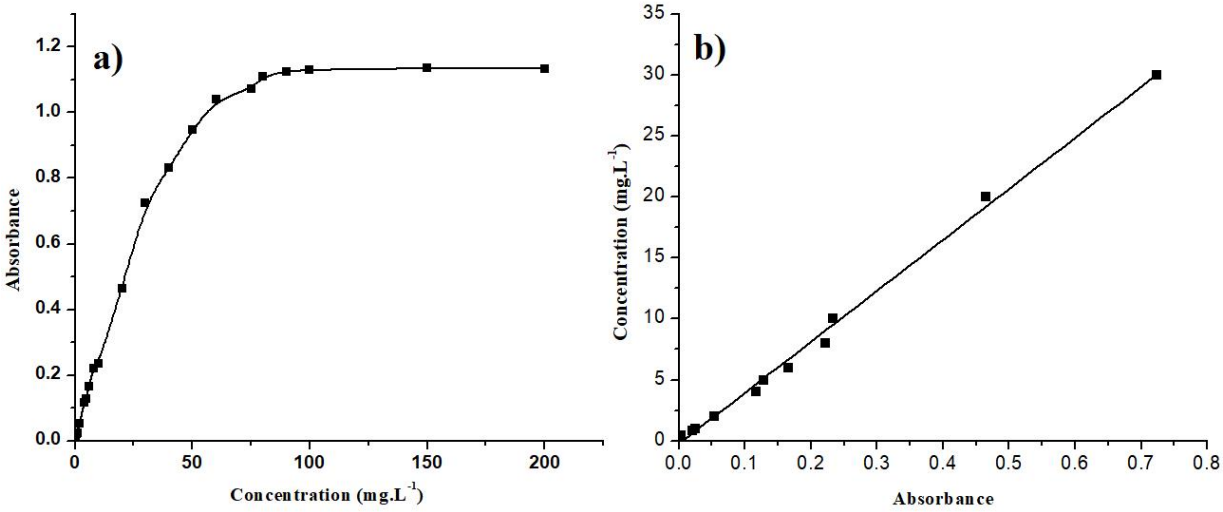

Figure 6 - Standard curve for quinoline absorbance vs concentration in 2,2,4 trimethylpentane and ethanol a) quinoline saturation curve, b) quinoline calibration curve.

As the values of R^2 is 0.996 very close to 1 and the 12 points of calibration have a good adjust. This result allows the quantification of quinoline concentration from the absorbance of the sample. The standard curve was made with only 12 points that vary its concentration from 0.2 to 30 mg·L^{-1}, because from this concentration the curve begins to saturate. The adsorption capacities were calculated for the Eq. (9).

$$q_t = \frac{(C_0 - C_t)\,V}{W} \tag{9}$$

When q_t represents the amount of quinoline adsorbed in the solid phase at time t (mg·g^{-1}), C_0 and C_t are the initial concentrations and time t of quinoline in the solution (mg·L^{-1}), respectively, V is the volume of solution (L) and W is the mass of biochars used (g).

3.6 KINETIC AND ISOTHERM ADSORPTION MODELS

The kinetic data were adjusted to the pseudo-first order and pseudo-second order models, according to the equations 4 and 6 that can be found in section 2.4.3 in its non-linearized form. The adjustment of the models was done through the Excel program with the use of the *solver* tool, or the minimization of the error and determination of pseudo-

first order and pseudo-second order constants. The model adjustment was evaluated through the determination coefficient (R^2) for all concentrations analyzed.

Similarly, the adsorption isotherms data were fitted to the Langmuir and Freundlich models according to the equations 1 and 2 that can be found in section 2.4.2. The model adjustment was evaluated through the determination coefficient (R^2) for all concentrations analyzed.

The kinetic models were used in their non-linear form, due to the fact that according to the literature they present a better fit of the data, because there are no problems with the transformations of the nonlinear equations to linear forms, being also in the same error calculation structures. Therefore, it is more appropriate to use the nonlinear method to estimate the parameters involved in the kinetic equation. Also the non-linear method has the advantage that the error distribution is not changed as in the linear technique, since all kinetic parameters are fixed on the same axis as verified by *Kumar (2006)*[58].

RESULTS AND DISCUSSION

4 RESULTS AND DISCUSSION

4.1 ACIDITY AND BASICITY

The study of surface chemistry is necessary because it plays a key role in the removal of aromatic compounds. In this sense, the acidity or basicity of material can be directly related to its adsorption capacity, since it affects both the electrostatic and the dispersive interactions between adsorbates and adsorbents[59]. The study of surface chemistry was carried out according to the methodology explained in section 3.3. The results are summarized in the Table 5.

Table 5 - Acid and base properties of the biochar materials.

Biochar	Acidity ($\mu mol \cdot g^{-1}$)	Basicity ($\mu mol \cdot g^{-1}$)
C_1G_3	$556 \pm 3.4.10^{-5}$	$288 \pm 1.7.10^{-5}$
C_2G_2	$768 \pm 7.0.10^{-5}$	$513 \pm 5.3.10^{-5}$
C_3G_1	548 ± 0.0	$863 \pm 5.3.10^{-5}$

According to the results obtained (Table 5), the basic character surface groups were found in significant concentrations in the biochar C_3G_1. It has been found that with the increase of the glycerol ratio in the structure of the compounds the basic character of the biochars decreases.

It is also observed that the biochar C_2G_2 presents the greater acid character and the materials C_1G_3 and C_3G_1 have similar acidic surface groups. The acidic character of a material is proven to be related to the oxygen content in its structure. The higher the oxygen content, the more acidic is the aqueous dispersion of the material, giving the material properties of the cation exchangers[60]. In Table 4 it is reported the composition of the materials being the oxygen content represented along with the amount of ash in remaining composition. Due to the ratio between carbon and glycerol the biochar C_2G_2 presents a proportionality between these materials whereas in the other materials a smaller quantity of oxygen and a minor acid character is verified.

The greater presence of acidic functional groups in the C_2G_2 biochars is an important characteristic, since it provides a greater field of use of this material for the adsorption of quinoline that presents a *pKa* 4.9 (pH 7.3) and ionizes positively in solution[61].

4.2 KINETIC STUDY ON THE ADSORPTION OF QUINOLINE

The study of the kinetics of quinoline adsorption included the evaluation of the influence of the initial concentration of adsorbate (quinoline) and the performance of each adsorbent material. Results are presented in **Figure 7**. The concentrations used for the kinetic study ranged from 2 to 120 $mg \cdot L^{-1}$ as defined in section 3.2.1, these experiments were carried out at low concentrations.

The adsorption tests were carried out with the three types of biochars proposed to evaluate their capacity of adsorption of quinoline, with the objective of investigating the potential of these materials for the treatment of oily wastewater.

Observing the results presented in **Figure 7**, it is verified that the adsorption of quinoline by all adsorbent materials investigated is faster at the first 30 minutes of contact between the adsorbent and the solution. This fact can be verified because, at the beginning of the adsorption, there are a large number of empty sites of the adsorbent available for adsorption and after the occupation of these sites by the quinoline the adsorption of this pollutant becomes slower.

After 60 minutes of adsorption the equilibrium has already been reached for practically all the materials in the different concentrations studied. *Potenciano et al. (2017)*[20] who studied the adsorption of quinoline on dendê coal showiest that the adsorption equilibrium was reached after 120 minutes. *Ahmed and Ahmaruzzaman (2016)*[62] who studied the adsorption of quinoline on coconut shell coal showed that adsorption equilibrium was reached after 180 minutes.

Another parameter that can be analyzed on Figure 7 is the effect of the initial concentration of quinoline, where it is verified that in the higher initial concentration of quinoline, the higher tends to be the adsorption capacity (q_t) after reaching equilibrium, as can be seen that the highest adsorption capacity was obtained at the initial concentration of 120 ppm. The higher removal efficiency of quinoline was verified in the 5 $mg \cdot L^{-1}$ solution, where 79% of the quinoline was removed while in the 120 $mg \cdot L^{-1}$ solution only 8.85% of the quinoline was removed.

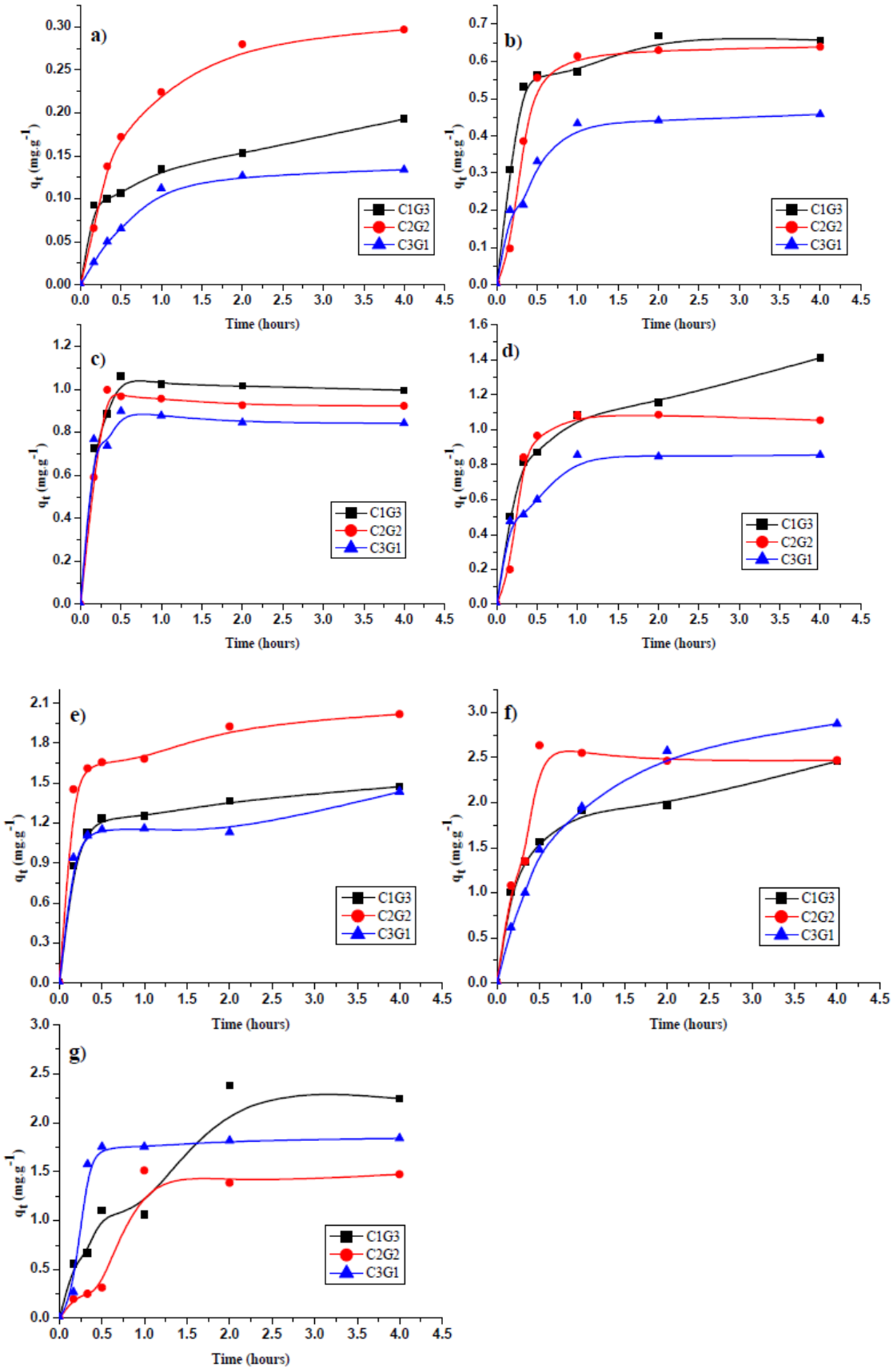

Figure 7 - Quinoline adsorption kinetics on activated carbons C1G3, C2G2 and C3G1 at 25 ºC initial quinoline concentration of (a) 2 mg·L^{-1}, (b) 5 mg·L^{-1}, (c) 10 mg·L^{-1}, (d) 25 mg·L^{-1}, (e) 50 mg·L^{-1}, (f) 75 mg·L^{-1} and (g) 120 mg·L^{-1}.

By analysing **Figure 7** it is verified that the biochars C_1G_3 and C_2G_2 presented better adsorption performance, because their adsorption capacity were the largest in all cases. This fact can be explained by the greater presence of mesoporous than microporous in the structure of these materials as verified by *Masso (2017)*[56], a fact that favours the adsorption of larger molecules such as quinoline. Although the biochar C_2G_2 possesses the same surface area as the biochar C_3G_1, this presents a low amount of mesoporous, fact that may have impaired the adsorption in this material. Of all the materials, the one that presents/displays greater amount of mesoporous is the biochar C_1G_3.

Rameshraja (2012)[63] who studied the adsorption of quinoline in granular activated carbon and fly ash from the bagasse obtained 93.5% and 98.3% removals, while *Ahmed and Ahmaruzzaman (2016)*[62] studied the adsorption of quinoline in bark activated carbon coconut and obtained a removal of 80.74 to 97.24%. *Saavedra* (2016)[21] that studied the adsorption of quinoline in polymers obtained maximum removals of 61.43%.

4.2.1 MODELLING THE KINETIC ADSORPTION OF QUINOLINE ON BIOCHARS

In order to study the kinetics of the reaction with each of the biochars, the modeling of the experimental adsorption data was carried out and, consequently, the choice of the model explaining the behavior of the system was performed by evaluating some statistical parameters obtained, as described in section 3.4. Figure 8 shows, respectively, the curves fitted to the kinetics of pseudo first order and pseudo second order in the non-linearized form, for all concentrations of quinoline studied and using the three biochar. The adjustments were based on the experimental data of q_e and q_t and using the equations Eq. 6 and Eq. 8.

*$qe_{,cal}$ expressed in $mg \cdot g^{-1}$, k_1 expressed in min^{-1} and k_2 expressed in $g \cdot mg^{-1} min^{-1}$

Table 7, Table 8 and Table 8 show the adjusted kinetic parameters for the quinoline adsorption process, as well as the values of the correlation coefficients (R^2).

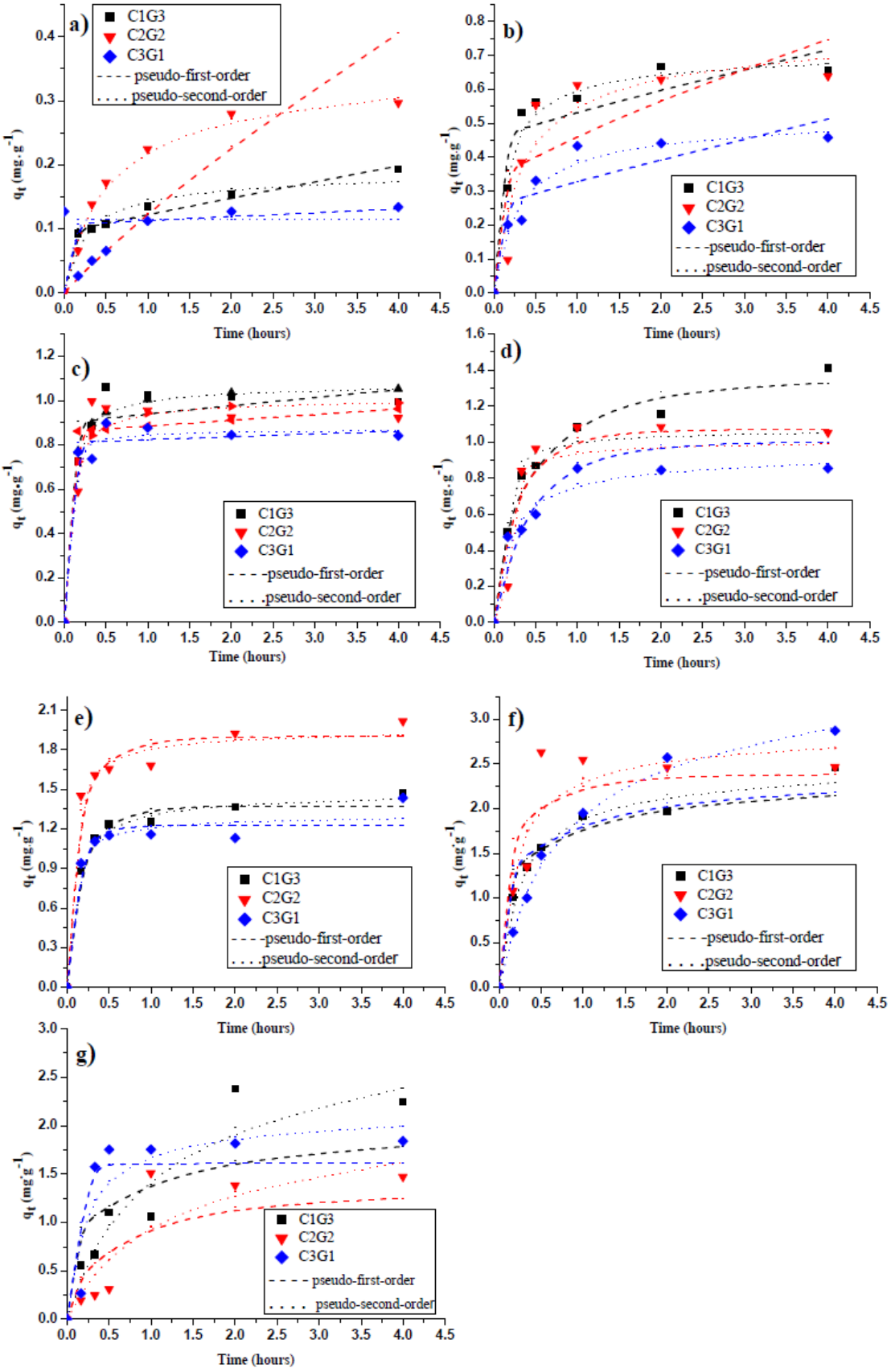

Figure 8 - Quinoline adsorption kinetics on activated carbons C_1G_3, C_2G_2 and C_3G_1 at 25 ºC initial quinoline concentration of (a) 2 mg·L^{-1}, (b) 5 mg·L^{-1}, (c) 10 mg·L^{-1}, (d) 25 mg·L-1, (e) 50 mg·L^{-1}, (f) 75 mg·L^{-1} and (g) 120 mg·L^{-1} and pseudo-first-orden and pseudo-secound-orden kinetic models.

Table 6 - Kinect parameters calculated from the pseudo-first-order and pseudo-second-order models to the experimental data of the adsorbent C1G3 at 25 ºC.

$C_{quinoline}$ (mg·L^{-1})	$q_{e,exp}$ (mg·g^{-1})	Pseudo-first-order	Pseudo-second-order
		$q_{e,cal}$ = 0.094	$q_{e,cal}$ = 0.184
2	0.309	k_1 = 4.54.10^{-4}	k_2 = 0.333
		R^2 = 0.961	R^2 = 0.840
		$q_{e,cal}$ = 0.460	$q_{e,cal}$ = 0.685
5	0.822	k_1 = 1.24.10^{-3}	k_2 = 0.152
		R^2 = 0.486	R^2 = 0.908
		$q_{e,cal}$ = 0,899	$q_{e,cal}$ = 1.068
10	0.943	k_1 = 6.69.10^{-4}	k_2 = 0.758
		R^2 = 0.176	R^2 = 0.999
		$q_{e,cal}$ = 0,331	$q_{e,cal}$ = 0.578
25	1.069	k_1 = 2.47.10^{-2}	k_2 = 6.503
		R^2 = 0.932	R^2 = 0.776
		$q_{e,cal}$ = 0.376	$q_{e,cal}$ = 1.462
50	1.428	k_1 = 6.69.10^{-2}	k_2 = 0.106
		R^2 = 0.898	R^2 = 0.955
		$q_{e,cal}$ = 1.170	$q_{e,cal}$ = 2.443
75	2.202	k_1 = 1.58.10^{-2}	k_2 = 0.0258
		R^2 = 0.93748	R^2 = 0.950
		$q_{e,cal}$ = 0.818	$q_{e,cal}$ = 3.018
120	2.648	k_1 = 1.44.10^{-2}	k_2 = 5.238.10^{-3}
		R^2 = 0.680	R^2 = 0.874

*$q_{e,cal}$ expressed in mg·g^{-1}, k_1 expressed in min^{-1}and k_2 expressed in g·mg^{-1} min^{-1}

Table 7 - Kinect parameters calculated from the pseudo-first-order and pseudo-second-order models to the experimental data of the adsorbent C2G2 at 25 ºC.

$C_{quinoline}$ (mg·L^{-1})	$q_{e,exp}$ (mg·g^{-1})	Pseudo-first-order	Pseudo-second-order
		$q_{e,cal}$ = 0.002	$q_{e,cal}$ = 0.344
2	0.304	k_1 = 1.91.10-2	k_2 = 0.090
		R^2 = 0.764	R^2 = 0.990
		$q_{e,cal}$ = 0.337	$q_{e,cal}$ = 0.750
5	0.690	k_1 = 2.20.10^{-3}	k_2 = 0.065
		R^2 = 0.423	R^2 = 0.840
		$q_{e,cal}$ = 0.857	$q_{e,cal}$ = 1.004
10	1.322	k_1 = 4.59.10^{-4}	k_2 = 0.257
		R^2 = 0.061	R^2 = 0,521
		$q_{e,cal}$ = 0.070	$q_{e,cal}$ = 0.271
25	1.033	k_1 = 5.23.10^{-2}	k_2 = 1.001
		R^2 = 0.875	R^2 = 0.984
		$q_{e,cal}$ = 0.90	$q_{e,cal}$ = 1.94
50	2.273	k_1 = 5.83.10^{-2}	k_2 = 0.130
		R^2 = 0.734	R^2 = 0.816
		$q_{e,cal}$ = 1.384	$q_{e,cal}$ = 2.817
75	2.037	k_1 = 3.33.10^{-2}	k_2 = 0.029
		R^2 = 0.705	R^2 = 0.711
		$q_{e,cal}$ = 0.262	$q_{e,cal}$ = 2.095
120	2.942	k_1 = 1.91.10^{-2}	k_2 = 6.78.10^{-3}
		R^2 = 0.863	R^2 = 0.817

*$q_{e,cal}$ expressed in mg·g^{-1}, k_1 expressed in min^{-1}and k_2 expressed in g·mg^{-1} min^{-1}

Table 8 - Kinect parameters calculated from the pseudo-first-order and pseudo-second-order models to the experimental data of the adsorbent C3G1 at 25 ºC.

$C_{quinoline}$ (mg·L^{-1})	$q_{e,exp}$ (mg·g^{-1})	Pseudo-first-order	Pseudo-second-order
2	0.810	$q_{e,cal}$ = 0.025 k_1 = 0.104 R^2 = 0.453	$q_{e,cal}$ = 0.869 k_2 = 0.776 R^2 = 0.844
5	0.336	$q_{e,cal}$ = 0.256 k_1 = 1.23.10^{-3} R^2 = 0.603	$q_{e,cal}$ = 0.511 k_2 = 0.107 R^2 = 0.920
10	0.810	$q_{e,cal}$ = 0.8105 k_1 = 2.19.10^{-4} R^2 =0.087	$q_{e,cal}$ = 0.870 k_2 = 0.776 R^2 = 0.705
25	0.600	$q_{e,cal}$ = 1.694 k_1 = 3.66.10^{-2} R^2 = 0,804	$q_{e,cal}$ = 0.924 k_2 = 0.088 R^2 = 0.887
50	0.929	$q_{e,cal}$ = 0.230 k_1 = 0.114 R^2 = 0.533	$q_{e,cal}$ = 1.299 k_2 = 0.194 R^2 = 0.650
75	2.555	$q_{e,cal}$ = 1.205 k_1 = 1.61.10^{-2} R^2 = 0.960	$q_{e,cal}$ = 3.441 k_2 =6.60.10^{-3} R^2 = 0.995
120	1,2868	$q_{e,cal}$ = 0.714 k_1 = 1.250 R^2 = 0.990	$q_{e,cal}$ = 2.112 k_2 = 3.307.10^{-2} R^2 = 0.691

*$q_{e,cal}$ expressed in mg·g^{-1}, k_1 expressed in min^{-1}and k_2 expressed in g·mg^{-1} min^{-1}

In the analysis of *qe,$_{cal}$ expressed in mg·g^{-1}, k_1 expressed in min^{-1}and k_2 expressed in g·mg^{-1} min^{-1}

Table 7, Table 8 and Table 8 and **Erro! Fonte de referência não encontrada.** it is possible to verify that the kinetic parameters that best fit the experimental data were those of pseudo-second-order for the three biochar tested, because they presented higher values of R^2 ranging from 0.685 to 0.999 and smaller discrepancies between quantity adsorbed in experimental equilibrium ($q_{e,exp}$) and calculated ($q_{e,cal}$). In this analysis, it is still possible to verify that the kinetic constant k_2 tends to decrease from 0.840 to 5.238.10^{-3} g·mg^{-1} min^{-1} for the biochar C_1G_3, from 0.090 to 6.78.10^{-3} g·mg^{-1} min^{-1} for the biochar C_2G_2 and from 0.776 to 3.307.10^{-2} g·mg^{-1} min^{-1} for the biochar $C3G_1$ by increasing solution concentration, proving that the adsorption efficiency is better at low concentration.

In the case of quinoline adsorption on activated carbon, the second-order model is better fitted to the data as reported by *Rameshraja (2012)*[63], who studied the adsorption

of quinoline in granular activated carbon and fly ash from the bagasse and obtained kinetic constant k_2 varying from 0.001 to 0.004 $g \cdot mg^{-1}$ min^{-1}. *Ferreira (2017)*[64] investigated adsorption of nitrogen compounds using activated carbon and obtained a kinetic constant k_2 of 0.009 for your best simulation.

4.3 EQUILIBRIUM STUDY

The study of the adsorption equilibrium was carried out in order to evaluate the maximum amount of quinoline that could be removed from the solution and the adsorption mechanism for each type of biochar used as adsorbent. The adsorption were carried out during 72 h.

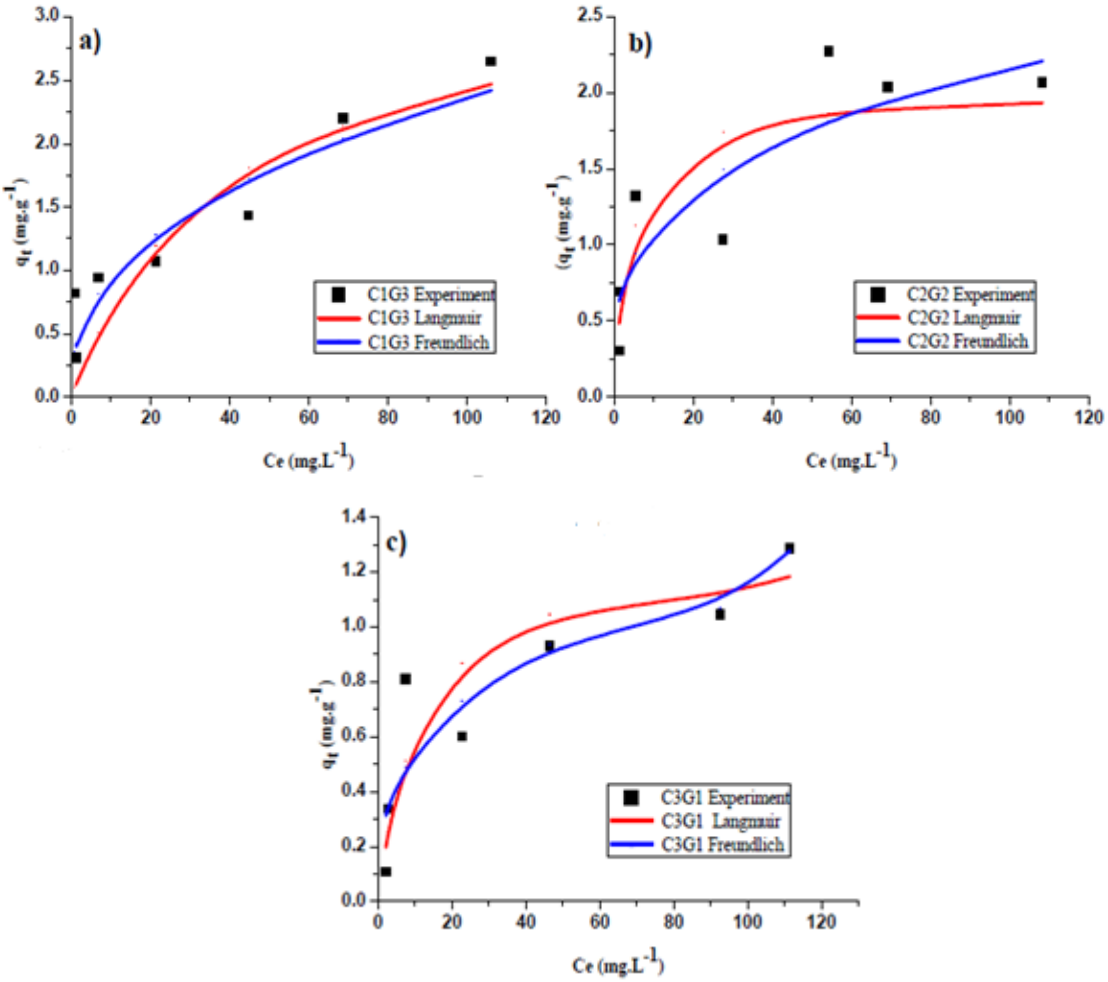

Figure 9 - Isotherms Biochar a) C_1G_3, b) C_2G_2 and c) C_3G_1.

It can be observed a behavior of the isotherms of type L, according to the classification proposed by *Giles et al. (1960)*[40] (Figure 3). The initial downward curvature indicates a decrease in the availability of active sites with the increase of the concentration of the solution and because it is concave, the isotherms indicate that the adsorption process is favorable[41]. Also according to the *Giles et al. (1960)*[40] classification, the isotherms cover subgroup 4, which indicates the formation of adsorbed multiple layers. The parameters obtained for the simulated Langmuir and Freundlich models for the adsorbents are shown in Table 9.

Table 9 - Parameters of the different non-linear models for adsorption of quinoline on activated carbon.

Adsorbent	Langmuir parameters	Freundlich parameters
C1G3	q_m = 3.376 mg·g^{-1} K_L = 0.026 L·mg^{-1} R^2 = 0.871	n = 2.473 K_F = 0.377 mg·g^{-1}(mg·L^{-1})$^{-1/n}$ R^2 = 0.895
C2G2	q_m = 2.058 mg·g^{-1} K_L = 0.227 L·mg^{-1} R^2 = 0.767	n = 3.429 K_F = 0.574 mg·g^{-1}(mg·L^{-1})$^{-1/n}$ R^2 = 0.797
C3G1	q_m = 1.027 mg·g^{-1} K_L = 0.166 L·mg^{-1} R^2 = 0.811	n = 3.432 K_F = 0.277 mg·g^{-1}(mg·L^{-1})$^{-1/n}$ R^2 = 0.841

Analyzing the correlation coefficients (R^2) of . **Table 9** together with the graphical interpretation of

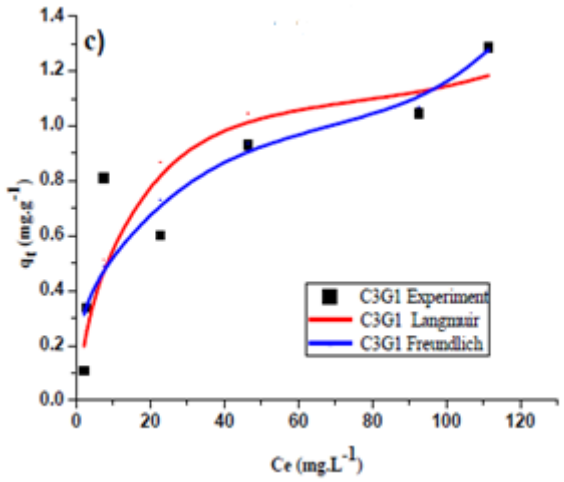

Figure **9**, the Freundlich model fit better the experimental data than Langmuir model.

The parameter *n* of the Freundlich model indicates how the energy of the sites are distributed. The value of *n* greater than 1 is an indication that quinoline adsorption is

favorable and that the sites are energetically heterogeneous, and highly energetic sites are likely to be occupied first than the less energetic ones. The obtained values of *n* indicate that the adsorption of the quinoline can be occurring by physisorption, with formation of multilayers[65].

The affinity relation between the adsorbent (quinoline) and the adsorbent (activated carbon) can be related by means of the adsorption constant of Freundlch k_F, which should always be analyzed in conjunction with parameter *n*. According[64] *Ferreira, (2014)* to high values of k_F and n indicate high adsorption in the concentration range studied, and conversely.

Other authors such as *Ferreira, (2014)*[64] and *Rameshraja et al.* (2018)[24] and that studied the adsorption of quinoline in activated carbon also verified in these works that the Freundlich isotherm presented better adjustments to the experimental data than the Langmuir isotherm.

The parameter q_m of the Langmuir model indicates the maximum adsorption capacity of the quinoline by the adsorbent and can be used to compare its efficiency and it is verified that the best adsorbent is the activated carbon C_1G_3 having the maximum adsorption capacity of 3.38 $mg \cdot L^{-1}$, however the adsorption capacity of the C_2G_2 material does not present a very significant difference.

Feng et al. (2005)[66], who evaluated the adsorption of quinoline solubilized in heptane using activated carbon chemically oxidized with ammonium persulfate, obtained a maximum adsorption capacity by the Langmuir model of 37.5 $mg \cdot g^{-1}$. *Li et al. (2011)* that studied the adsorption of quinoline, using decane as solvent, in thirteen activated carbon, obtained in their best adsorbent q_{max} equal to 29.4 $mg \cdot g^{-1}$.

Since the adsorption capacity of a material is directly linked to its surface area, the low adsorption capacity of the activated carbons used can be justified by the low surface area of these materials, as shown in Table 4, when compared to the commercial activated carbon with have a surface area that varies between[67] 800 and 5000 $m^2 \cdot g^{-1}$⁶⁷⁶⁷⁶⁷ that is, 57 to 357 times greater than the material used. However, it is important to mention that the biochar used were synthesized from urban waste and therefore these materials can be considered viable adsorbents, since they give a noble destination for these materials, besides enabling the production of activated coals of relatively lower cost, when compared to commercial activated carbons.

CONCLUSIONS AND FUTURES RESEARCH

5 CONCLUSIONS AND FUTURE RESEARCH

5.1 CONCLUSIONS

In this work the removal of quinoline, a nitrogen contaminant present in several petroleum fractions, using different biochars was studied. At the end of this work it was verified that of the biochars studied the ones that presented better performance were the materials C_1G_3 and C_2G_2, due to its surface properties more favorable to the adsorption the presence of acid groups in its surface.

By means of kinetic studies, it was also verified that an increase of the quinoline initial concentration results in a higher value of q_e, however the reduction of the adsorption velocity occurs, which is verified in the reduction of quinoline removal efficiency, and these materials are able to remove efficiently lower amounts of quinoline of the organic phase.

Biochars can be used as adsorbents for oily wastewater that does not have high concentrations of contaminants, mainly because they are synthesized from urban waste presenting low production costs.

5.2 FUTURE RESEARCH

For future studies of adsorption of quinoline in the biochars C_1G_3, C_2G_2 and C_3G_1 is interesting to evaluate the conditions that would be considered optimal for the adsorption process to make it more efficient. This study would be developed by analyzing the adsorption efficiency of quinoline when properties such as pH of adsorption medium, temperature, amount of adsorbent and phases where adsorption occurs are modified.

In addition, the study of the use of these materials for the removal of quinoline by means of other processes of treatment of waste water as a process of peroxide catalytic oxidation (CWPO).

REFERENCES

REFERENCEs

1. Aljuboury DADA, Palaniandy P, Abdul Aziz HB, Feroz S. Treatment of petroleum wastewater by conventional and new technologies - A review. *Glob Nest J*. 2017;19(3):439-452.

2. Gryta M, Karakulski K, Morawski AW. PURIFICATION OF OILY WASTEWATER BY HYBRID UF / MD. 2001;35(15):3665-3669.

3. Yu L, Han M, He F. A review of treating oily wastewater. *Arab J Chem*. 2013;10:S1913-S1922.

4. Diaz de Tuesta JL, Silva AMT, Faria JL, Gomes HT. Removal of Sudan IV from a simulated biphasic oily wastewater by using lipophilic carbon adsorbents. *Chem Eng J*. 2018;347(April):963-971.

5. Damasceno L. TRATAMENTO DE ÁGUAS OLEOSAS ORIUNDAS DO PROCESSO DE PRODUÇÃO DE ÓLEO DE DENDÊ UTILIZANDO A FLOTAÇÃO POR AR DISSOLVIDO. *Diss (Trabalho conclução curso Eng Ambient Univ Estadual Paul Campinas*. 2009.

6. Zhou YB, Tang XY, Hu XM, Fritschi S, Lu J. Emulsified oily wastewater treatment using a hybrid-modified resin and activated carbon system. *Sep Purif Technol*. 2008;63(2):400-406.

7. Hamdaoui O, Naffrechoux E. Modeling of adsorption isotherms of phenol and chlorophenols onto granular activated carbon. Part I. Two-parameter models and equations allowing determination of thermodynamic parameters. *J Hazard Mater*. 2007;147(1-2):381-394.

8. Marques J, Rangel C. PROCESSOS AVANÇADOS DE OXIDAÇÃO DE COMPOSTOS FENÓLICOS EM EFLUENTES INDUSTRIAIS. *Quim Nov*. 2008;31(1):114-122.

9. Amoatey P, Bani R, Richard Bani P. Wastewater Management 20 Wastewater Management. 2011;(February):379-398.

10. Gomes EA. Tratamento combinado da água produzida de petróleo por

eletroflotação e processo fenton. *Diss (Mestrado em Eng Process Univ Tiradentes, Aracaju*. 2009:95. doi:G633t

11. Fakhru'l-Razi A, Pendashteh A, Abdullah LC, Biak DRA, Madaeni SS, Abidin ZZ. Review of technologies for oil and gas produced water treatment. *J Hazard Mater*. 2009;170(2-3):530-551.

12. Hui L, Yan W, Juan W, Zhongming L. A review: Recent advances in oily wastewater treatment. *Recent Innov Chem Eng*. 2014;7(1):17-24.

13. H. Elhussien M. Preparation and Characterization of Activated Carbon from Palm Tree Leaves Impregnated with Zinc Chloride for the Removal of Lead (II) from Aqueous Solutions. *Am J Phys Chem*. 2017;6(4):59.

14. Sum J, Aprova RIO, Europeu P, Aprova D, Europeu P, Europeu P. Lei da água. 2019:1-35.

15. Wang X, Huang X, Zuo C, Hu H. Kinetics of quinoline degradation by O3/UV in aqueous phase. *Chemosphere*. 2004;55(5):733-741. doi:10.1016/j.chemosphere.2003.11.019

16. PETRÓLEO DDMEPDDCNECD DO. Okumura, L.L. *Diss (Doutorado em Química) Unversidade Estadual Pailista*. 2008;Araraquara.

17. Draft F. TOXICOLOGICAL REVIEW OF. *Rev Lit Arts Am*. 2005;(91).

18. Thomsen AB. Degradation of quinoline by wet oxidation - Kinetic aspects and reaction mechanisms. *Water Res*. 1998;32(1):136-146.

19. Thomsen AB, Kilen HH. Wet oxidation of quinoline: Intermediates and by-product toxicity. *Water Res*. 1998;32(11):3353-3361. doi:10.1016/S0043-1354(98)00116-X

20. Potenciano NFF, Ferreira MEO, Alonso CG, Ostroski IC. Estudo Cinético da Adsorção de Quinolina em Carvão Ativado de Casca de Dendê Funcionalizado Quimicamente Metodologia A quantidade de quinolina adsorvida foi calculada pelo. 2017:77-81.

21. Saavedra LNM. Sínteses de polímeros molecularmente impressos para adsorção seletiva de quinolina em matriz orgânica. 2017:124.

22. Luvas U, Fogo RAO. Quinolina. :1-3.

23. Chong MN, Jin B, Chow CWK, Saint C. Recent developments in photocatalytic water treatment technology: A review. *Water Res*. 2010;44(10):2997-3027.

24. Rameshraja D, Srivastava VC, Kushwaha JP, Mall ID. Competitive adsorption isotherm modelling of heterocyclic nitrogenous compounds, pyridine and quinoline, onto granular activated carbon and bagasse fly ash. *Chem Pap*. 2018;72(3):617-628.

25. Ho YS, McKay G. Pseudo-second order model for sorption processes. *Process Biochem*. 1999;34(5):451-465. doi:10.1016/S0032-9592(98)00112-5

26. Salahshoor Z, Shahbazi A. Review of the use of mesoporous silicas for removing dye from textile wastewater. *Eur J Environ Sci*. 2014;4(2):116-130.

27. Piva JALD, Santos O, Andrade CMG. Determinação e análise de isotermas de adsorção do corante azul 5G em leito fixo de carvão ativado. *Acta Sci Technol*. 2011;33(4):435-438.

28. Liu QS, Zheng T, Wang P, Jiang JP, Li N. Adsorption isotherm, kinetic and mechanism studies of some substituted phenols on activated carbon fibers. *Chem Eng J*. 2010;157(2-3):348-356.

29. Petroni S. Avaliação cinética e de equilíbrio do processo de adsorção dos íons dos metais cádmio, cobre e níquel em turfa. *Diss (Doutorado0*. 2004:134.

30. Schneider EL. Adsorção de compostos fenólicos sobre carvão ativado Adsorção de compostos fenólicos sobre carvão ativado. *Dissetação (Mestrado em Eng Química), Univ Estadual do Oeste do Paraná, Toledo*. 2008.

31. Nascimento, R. F; Lima, A. C. A; Vidal, C. B; Melo, D. de Q; Raulino GSC. *Adsorção Aspectos Teóricos e Aplicações Ambientais*.; 2014.

32. Porpino KK. Biossorçao de Ferro (II) por casca de caranguejo Ucides cordatus. *Diss (Mestrado em Química), Univ Fed da Paraíba, João PEssoa*. 2009;(Ii):93.

33. Borba CE. Modelagem da remoção de metais pesados em coluna de adsorção le leito fixo. *Diss (Mestrado em Eng Process Univ Campinas*. 2006;Campinas.

34. Farias Oliveira R. Estudo da adsorção de Cr (VI) em altas concentrações. *Diss*

(Mestrado em Eng Química), Univ Fed do Rio Gd do Sul, Porto Alegre. 2013.

35. Muranaka NT. Combinação de adsorção por carvão ativado com Processo Oxidativo Avançado (POA) para tratamento de efluentes contendo Fenol. *Tese Doutorado*. 2010:165.

36. Medeiros SHW. Estudo Da Cinética De Adsorção De S02 Em Sistema De Leito Fluidizado. 2001:182.

37. Isabel T, Duarte M. Espectroscopia in situ no estudo cinético da adsorção de produtos farmacêuticos poluentes em carvões activados. *Diss (Mestr em Eng Química e Bioquímica), Univ Lisboa*. 2014. https://run.unl.pt/bitstream/10362/13826/1/Duarte_2014.pdf.

38. Lopes AR. Adsorção de compostos de enxofre e nitrôgenio do diesel comercial por carvão ativado impregnado com paládio. *Diss (Doutorado em Eng e Ciência dos Mater Univ Fed do Paraná*. 2014;Curitiba:561-565.

39. Letterman S. Adsorção. *Pontifícia Univ Católica Rio Janeiro (PUC- Rio)*. 1999:43-58.

40. Giles CH, D'Silva AP, Easton IA. A general treatment and classification of the solute adsorption isotherm part. II. Experimental interpretation. *J Colloid Interface Sci*. 1974;47(3):766–778.

41. Zago S, Maria E. Adsorção/Dessorção do explosivo tetril em turfa e em argissolo vermelho amarelo. *Quim Nova*. 2004;27(6):849-854.

42. Petriciolet AB, Castillo DIM ÁH. Adsorption Processes for Water Treatment and Purification. Springer Link.

43. Castro CS de. Preparação de carvão ativado a partir de borra de café: uso como adsorvente e como suporte catalítico para a remoção de poluentes orgânicos em meio aquoso. *Diss (Mestrado em Agroquímica), Univ Fed Lavras*. 2009:92.

44. ALLEONI LRF, CAMARGO OA, CASAGRANDE JC. Isotermas de langmuir e de freundlich na descrição da adsorção de boro em solos altamente intemperizados. *Sci Agric*. 2005;55(3):379-387.

45. Linhares LA, Filho FBE, Bellis VM de, Santos EA dos, Ianhez R. Utilização dos

modelos de Langmuir e de Freundlich na adsorção de cobre e zinco em solos Brasileiros. *Acta Agronómica*. 2010;59(3):303-315.

46. Souza RS, Chaves LHG, Fernandes JD. Isotermas de Langmuir e de Freundlich na descrição da adsorção de zinco em solos do Estado da Paraíba 1 Langmuir and Freundlich isotherms to describe zinc adsorption by soils from. *Rev Bras ciencias Agrar*. 2007;2:123-127.

47. GOMES DAA. Adsorção De N-Parafinas Na Faixa De C10 a C13 Sobre Adsorção De N-Parafinas Na Faixa De C10 a C13 Sobre. *Diss (Doutorado em Eng Química), Univ Fed da Bahia, Salvador*. 2014:113.

48. Luís PM dos S de S. Remoção de cor em efluentes têxteis por adsorção em ma. *TDissertação (Mestrado em Eng Química) Univercidade do Porto*. 2009:221.

49. Masel RI. Principles of adsorption and reaction on solid surfaces. *Wiley Ser Chem Eng*. 1996:xiv, 804 p.

50. Kyzas GZ, Kostoglou M. Green adsorbents for wastewaters: A critical review. *J Mater*. 2014;7(1):333-364.

51. Pommerening N. Utilização de diferentes materiais como adsorventes na remoção de nitrogênio amoniacal. *Diss (Mestr em Eng Ambient Univ Fed St Maria*. 2015:148.

52. González-García P. Activated carbon from lignocellulosics precursors: A review of the synthesis methods, characterization techniques and applications. *Renew Sustain Energy Rev*. 2018;82:1393-1414. http://dx.doi.org/10.1016/j.rser.2017.04.117.

53. Junior G de CM. CARVÃO ATIVADO Uso no tratamento de água. *Diss (Mestr em Eng Civel), Pontíifícia Univ Católica Belo Horiz*. 2010:2-25.

54. Mucciacito J. Uso eficiente do carvão ativado como meio filtrante em processos industriais. http://www.meiofiltrante.com.br/edicoes.asp?id=502&link=ultima&fase=C&retorno=c.

55. FERREIRA JCR. REMOÇÃO DE MICROPOLUENTES EMERGENTES EM EFLUENTES SANITÁRIOS ATRAVÉS DE CARVÃO ATIVADO. *Diss*

(Mestrado em Meio Ambient Urbano e Ind Univ Fed do Paraná. 2011;Curitiba.

56. Masso CM. Valorization of compost in the production of carbon-based materials for the treatment of contaminated wastewater Valorization of compost in the production of carbon-based materials for the treatment of contaminated wastewater. *Mestr IPB*. 2018.

57. Ribeiro RS, Silva AMT, Figueiredo JL, Faria JL, Gomes HT. Removal of 2-nitrophenol by catalytic wet peroxide oxidation using carbon materials with different morphological and chemical properties. *Appl Catal B Environ*. 2013;140-141:356-362. doi:10.1016/j.apcatb.2013.04.031

58. Kumar KV. Linear and non-linear regression analysis for the sorption kinetics of methylene blue onto activated carbon. *J Hazard Mater*. 2006;137(3):1538-1544.

59. Silva MV. Adsorção De Cromo Hexavalente Por Carvão Ativado Granulado Comercial Na Presencia De Surfatante Anionico. *Diss (mestrado em Eng Química) Univ Fed do Pará*. 2012;Belém:80.

60. Da Silva Guimarães I. oxidação de carvões ativados de endorcarpo de coco da baía com solucoesde HNO3 e uma investigação sobre o metodo de Boehm. *Diss (Mestrado em Química) Univ Fed da Paraíba*. 2006.

61. Marella A, Tanwar OP, Saha R, et al. Quinoline: A versatile heterocyclic. *Saudi Pharm J*. 2013;21(1):1-12. http://dx.doi.org/10.1016/j.jsps.2012.03.002.

62. Ahmed MJK, Ahmaruzzaman M. Investigation on the effective remediation of quinoline at solid/solution interface using modified agricultural waste: an inclusive study. *Int J Environ Sci Technol*. 2016;13(4):1177-1188.

63. Rameshraja D, Srivastava VC, Kushwaha JP, Mall ID. Quinoline adsorption onto granular activated carbon and bagasse fly ash. *Chem Eng J*. 2012;181-182:343-351.

64. Ferreira ME de O. Adsorção de compostos nitrogenados utilizando carvão atiado. *Diss (Química Agroindustrial), Univ Fed do Goiás*. 2017.

65. McCABE, W. L.; SMITH, J. C.; HARRIOTT, P. Unit Operations of Chemical Engineering, 6a ed., Editora McGraw-Hill, 1114 p, 2001. 2001:2001.

66. FENG, X.; MA, X.; LI, N.; SHANG, C.; YANG, X.; CHEN XD. Adsorption of quinoline from liquid hydrocarbons on graphite oxide and activated carbons. *Rsc Adv*. 2015;5(91):74684– 74691.

67. PEGO MFF. Modificação Superficial De Carvão Ativado Utilizando Tratamento Corona. *Diss (Mestr em Ciência eTecnologia da Madeira), Univ Fed Lavra, Lavras*. 2016.

ATTACHMENTS

Table 1 - Linear kinect parameters calculated from the pseudo-first-order and pseudo-second-orden models to the experimental data of the adsorbent C_1G_3 at 25 ºC.

Initial concentration ($mg \cdot L^{-1}$)	**$q_{e,exp}$ ($mg \cdot g^{-1}$)**	**Pseudo-first-orden**	**Pseudo-second-orden**
2	0.3093	$q_{e.cal}$ = 0.2171 k_1 = 0.0026 R^2 = 0.9834	$q_{e.cal}$ = 0.2054 k_2 = 0.1958 R^2 = 0.9852
5	0.8220	$q_{e.cal}$ = 0.3398 k_1 = 0.0038 R^2 = 0.5897	$q_{e.cal}$ = 0.6848 k_2 = 0.761 R^2 = 0.9982
10	0.9428	$q_{e.cal}$ = 0.9148 k_1 = 0.05734 R^2 = 1	$q_{e.cal}$ = 1.0050 k_2 = 1.1605 R^2 = 0.9992
25	1.0698	$q_{e.cal}$ = 0.8706 k_1 = 0.0523 R^2 = 0.9141	$q_{e.cal}$ = 1.5010 k_2 = 0.0298 R^2 = 0.9930
50	1.4282	$q_{e.cal}$ = 0.4615 k_1 = 0.01691 R^2 = 0.8958	$q_{e.cal}$ = 1.5116 k_2 = 0.0758 R^2 = 0.9987
75	2.2024	$q_{e.cal}$ = 1.076 k_1 = 0.01454 R^2 = 0.8456	$q_{e.cal}$ = 2.5957 k_2 = 0.0182 R^2 = 0.9901
120	2.6487	$q_{e.cal}$ = 1.9840 k_1 = 0.0083 R^2 = 0.6796	$q_{e.cal}$ = 2.8501 k_2 = 0.0061 R^2 = 0.9151

*$q_{e.cal}$ expressed in $mg \cdot g^{-1}$. k_1 expressed in min^{-1} and k_2 expressed in $g \cdot mg^{-1}\ min^{-1}$

Table 210- Linear kinect parameters calculated from the pseudo-first-order and pseudo-second-orden models to the experimental data of the adsorbent C_2G_2 at 25 ºC.

Initial concentration ($mg \cdot L^{-1}$)	$q_{e \cdot exp}$ ($mg \cdot g^{-1}$)	Pseudo-first-orden	Pseudo-second-orden
2	0.3046	$q_{e.cal}$ = 0.2124 k_1 = 0.01457 R^2 = 0.9674	$q_{e.cal}$ = 0.3410 k_2 = 0.0906 R^2 = 0.9960
5	0.6906	$q_{e.cal}$ = 0.2652 k_1 = 0.008452 R^2 = 0.5853	$q_{e.cal}$ = 0.7313 k_2 = 0.0518 R^2 = 0.9461
10	1.3223	$q_{e.cal}$ = 0.9278 k_1 = 2.1600 R^2 = 0.0313	$q_{e.cal}$ = 0.6946 k_2 = 0.0002 R^2 = 0.9990
25	1.0336	$q_{e.cal}$ = 2.7042 k_1 = 0.1249 R^2 = 0.9895	$q_{e.cal}$ = 1.1596 k_2 0.0523 R^2 = 0.9629
50	2.2728	$q_{e.cal}$ = 0.7511 k_1 = 0.0048 R^2 = 0.9985	$q_{e.cal}$ = 2.0658 k_2 = 0.0638 R^2 = 0.9302
75	2.0376	$q_{e.cal}$ = 1.3325 k_1 = 0.0331 R^2 = 1	$q_{e.cal}$ = 2.5865 k_2 = 0.0464 R^2 = 0.9928
120	6.9418	$q_{e.cal}$ = 1.6076 k_1 = 0.0050 R^2 = 0.5920	$q_{e.cal}$ = 2.4760 k_2 = 0.0030 R^2 = 0.6747

*$q_{e.cal}$ expressed in $mg \cdot g^{-1}$. k_1 expressed in $min^{-1}$and k_2 expressed in $g \cdot mg^{-1}\ min^{-1}$

Table 3 - Linear kinect parameters calculated from the pseudo-first-order and pseudo-second-orden models to the experimental data of the adsorbent C_3G_1 at 25 ºC.

Initial concentration ($mg \cdot L^{-1}$)	$q_{e \cdot exp}$ ($mg \cdot g^{-1}$)	Pseudo-first-orden	Pseudo-second-orden
2	0.8100	$q_{e.cal}$ = 0.0247 k_1 = 0.0541 R^2 = 1	$q_{e.cal}$ = 0.8443 k_2 = 15.3528 R^2 = 0.9995
5	0.3367	$q_{e.cal}$ = 0.0523 k_1 = 0.0036 R^2 = 0.0686	$q_{e.cal}$ = 0.4922 k_2 = 0.1278 R^2 = 0.9955
10	0.8100	$q_{e.cal}$ = 0.0247 k_1 = 0.0541 R^2 = 9995	$q_{e.cal}$ = 0.8443 k_2 = 15.352 R^2 = 1
25	0.5996	$q_{e.cal}$ = 1.6940 k_1 = 0.114 R^2 = 0.8049	$q_{e.cal}$ = 0.8985 k_2 = 0.1070 R^2 = 0.9971
50	0.9294	- - -	$q_{e.cal}$ = 1.4374 k_2 = 0.0629 R^2 = 0.9833
75	2.5548	$q_{e.cal}$ = 2.3920 k_1 = 0.0235 R^2 = 1	$q_{e.cal}$ = 3.4253 k_2 = 0.0066 R^2 = 0.9983
120	1.2868	$q_{e.cal}$ = 0.9390 k_1 = 0.0038 R^2 = 0.9313	$q_{e.cal}$ = 2.0783 k_2 = 0.0207 R^2 = 0.1910

*$q_{e.cal}$ expressed in $mg \cdot g^{-1}$. k_1 expressed in $min^{-1}$and k_2 expressed in $g \cdot mg^{-1}\ min^{-1}$

Table 4 - Parameters of the different linear and non-linear models for adsorption of quinoline on activated carbon.

Adsorventes	Linear Langmuir parameters	Non linear Langmuir parameters	Linear Freundlich parameters	Non lianear Freundlich parameters
	$q_m = 2.766^a$	$q_m = 3.376^a$	n = 3.088	n = 2.473
C_1G_3	$K_L = 0.056^b$	$K_L = 0.026^b$	$K_F = 0.489^c$	$K_F = 0.377^c$
	$R^2 = 0.871$	$R^2 = 0.876$	$R^2 = 0.758$	$R^2 = 0.895$
	$q_m = 2.253^a$	$q_m = 2.058^a$	n = 3.521	n = 3.429
C_2G_2	$K_L = 0.108^b$	$K_L = 0.227^b$	$K_F = 0.467^c$	$K_F = 0.574^c$
	$R^2 = 0.733$	$R^2 = 0.767$	$R^2 = 0.767$	$R^2 = 0.797$
	$q_m = 1.602^a$	$q_m = 1.027^a$	n = 2.061	n = 2.868
C_3G_1	$K_L = 5.862^b$	$K_L = 0.166^b$	$K_F = 0.150^c$	$K_F = 0.241^c$
	$R^2 = 0.782$	$R^2 = 0.787$	$R^2 = 0.726$	$R^2 = 0.822$

a = $mg \cdot g^{-1}$. b = $L \cdot mg^{-1}$. c = $mg \cdot g^{-1}(mg \cdot L^{-1})^{-1/n}$